3-30-2007

Effect of Ferroelectricity on Electron Transport in Pt/BaTiO$_3$/Pt Tunnel Junctions

Julian P. Velev
University of Nebraska-Lincoln, julian.velev@unl.edu

Chun-gang Duan
University of Nebraska-Lincoln, cgduan@clpm.ecnu.edu.cn

Kirill D. Belashchenko
University of Nebraska-Lincoln, belashchenko@unl.edu

Sitaram Jaswal
University of Nebraska, sjaswal1@unl.edu

Evgeny Y. Tsymbal
University of Nebraska-Lincoln, tsymbal@unl.edu

Effect of Ferroelectricity on Electron Transport in Pt/BaTiO$_3$/Pt Tunnel Junctions

J. P. Velev, Chun-Gang Duan, K. D. Belashchenko, S. S. Jaswal, and E. Y. Tsymbal

*Department of Physics and Astronomy, Nebraska Center for Materials and Nanoscience, University of Nebraska,
Lincoln, Nebraska 68588, USA*

Based on first-principles calculations, we demonstrate the impact of the electric polarization on electron transport in ferroelectric tunnel junctions (FTJs). Using a Pt/BaTiO$_3$/Pt FTJ as a model system, we show that the polarization of the BaTiO$_3$ barrier leads to a substantial drop in the tunneling conductance due to changes in the electronic structure driven by ferroelectric displacements. We find a sizable change in the transmission probability across the Pt/BaTiO$_3$ interface with polarization reversal, a signature of the electroresistance effect. These results reveal exciting prospects that FTJs offer as resistive switches in nanoscale electronic devices.

Thin film ferroelectrics have recently aroused significant interest due to their technological application in electronic devices such as ferroelectric memories [1,2]. One of the important characteristics affecting the performance of memory devices based on ferroelectric capacitors are leakage currents. Therefore, conduction through thin film ferroelectrics has been active area of research over the years (see, Refs. [1,2] for reviews). For films of hundred nanometer thickness it was found that transport mechanisms are similar to those known for wide band gap semiconductors. In particular, Schottky thermionic emission [3], Poole-Frenkel conduction [4], and Fowler-Nordheim tunneling [5] were considered as possible sources of leakage currents in ferroelectric capacitors.

This transport behavior changes dramatically when a film thickness approaches a nanometer scale, making direct tunneling the dominant mechanism of conduction [6]. Recent experimental [7–9] and theoretical [10–12] studies of perovskite ferroelectric oxides demonstrate that ferroelectricity persists down to a nanometer scale, which makes it possible to use ferroelectrics as tunnel barriers in ferroelectric tunnel junctions (FTJs) [6]. Based on simple models it was predicted that the reversal of the electric polarization of the ferroelectric barrier can produce a sizable effect on resistance of a FTJ [13,14]. Indications of such an electroresistance effect have been seen in experiments on Pt/Pb(Zr$_{0.52}$Ti$_{0.48}$)O$_3$/SrRuO$_3$ junctions [15]. Recently, the electroresistance effect was observed in FTJs utilizing a multiferroic La$_{0.1}$Bi$_{0.9}$MnO$_3$ barrier that exhibits the electrical resistance change with the reversal of the ferroelectric polarization [16]. This phenomenon is different from resistive switching which may also occur in thick ferroelectric barriers where the transport is not dominated by tunneling [17] and where it is not related to the reversal of ferroelectric polarization [18].

In this Letter we use first-principles calculations based on density functional theory to investigate intrinsic mechanisms responsible for the effect of the electric polarization of the barrier on electron tunneling in FTJs. We consider a Pt/BaTiO$_3$/Pt(001) FTJ as a model system to study this phenomenon. We predict that the polarization of the BaTiO$_3$ barrier leads to a substantial drop in the tunneling conductance due to changes in the electronic structure driven by ferroelectric displacements. We find a sizable change in the transmission probability across the Pt/BaTiO$_3$ interface with polarization reversal, a signature of the electroresistance effect.

Density functional calculations of the electronic and atomic structure of Pt/BaTiO$_3$ are performed within supercell geometry using the projector augmented wave method implemented in the Vienna *ab-initio* simulation package (VASP) [19,20] and a tight-binding linear muffin-tin orbital (TB-LMTO) method [21,22]. We consider a TiO$_2$-terminated interface with interfacial O atoms occupying atop sites on Pt. The in-plane lattice constant is fixed to be the experimental value of bulk BaTiO$_3$ (3.991 Å), [23] which is smaller than the theoretical lattice constant for the cubic phase of BaTiO$_3$ (4.033 Å) but larger than that of fcc Pt (3.976 Å). This produces a tetragonal distortion of both fcc Pt ($c/a = 0.99$) and BaTiO$_3$ ($c/a = 1.02$) structures. Thus, supercells in our calculations are (Pt$_2$)$_9$-TiO$_2$-(BaO-TiO$_2$)$_m$, where $m = 1$–8. Figure 1 shows the atomic structure of the $m = 4$ FTJ.
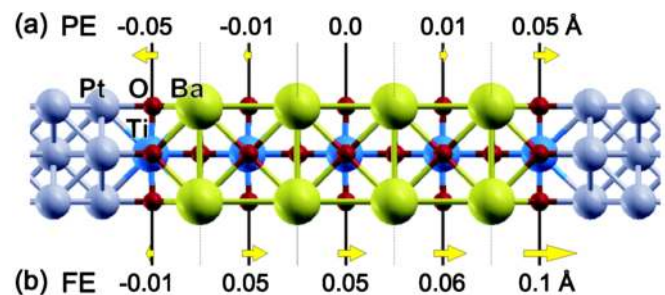

FIG. 1 (color online). Atomic structure of a Pt/BaTiO$_3$/Pt(001) tunnel junction. Arrows show displacements of Ti atoms with respect to O atoms within each TiO$_2$ monolayer for (a) paraelectric (PE) and (b) ferroelectric (FE) BaTiO$_3$.

137201-1

First, we assume that $BaTiO_3$ is in a paraelectric state. For this purpose we enforce reflection symmetry with respect to the central TiO_2 monolayer and relax the atomic structure of the whole system. We find that, although the net polarization of the $BaTiO_3$ film is zero, bonding at the interface induces displacements of the interface Ti atoms [Fig. 1(a)]. Then, we remove the constraint of reflection symmetry and minimize the total energy with respect to atomic coordinates of all atoms in the multilayer. For the $m = 2$ supercell, we obtain no ferroelectric instability. Thickness $t \approx 1$ nm of the $BaTiO_3$ film corresponding to $m = 2$ appears to be the critical value for ferroelectricity. Increasing the thickness up to $t \approx 1.8$ nm ($m = 4$) is sufficient for ferroelectric instability to develop [Fig. 1(b)]. For $m = 4$ the displacements of Ti atoms at the central TiO_2 monolayer are about 0.052 Å, which is less than the respective displacements in bulk $BaTiO_3$ (0.123 Å) by more than a factor of 2.

Figure 2(a) shows the local density of states (DOS) for the junction with a $m = 4$ $BaTiO_3$ barrier layer in a paraelectric state. The valence band of $BaTiO_3$ is primarily composed of the O-$2p$ states, whereas the conduction band is dominated by the Ti-$3d$ character. Figure 2(a) indicates that the band gap of the paraelectric $BaTiO_3$ is about 1.6 eV [24] which is seen from the distance between the valence band maximum (VBM) and the conductance band minimum (CBM) determined by the O bulk states. The Fermi level lies about 0.3 eV below the CBM.

Ferroelectric displacements produce notable changes in the electronic structure of a $Pt/BaTiO_3/Pt$ FTJ. It is seen from Fig. 2(b) that the local DOS for the Ti atoms at the left
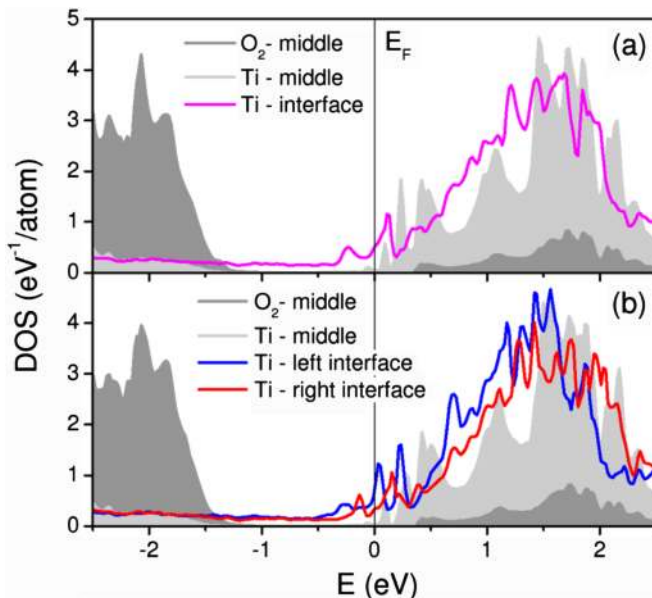
and right interfaces (distinguished by the polarization orientation, as in Fig. 1) are different. There is a rigid shift of about 0.2 eV in the local DOS caused by the dissimilar electrostatic potentials at the two interfaces. This effect is stronger than the potential change due to a depolarizing field, which is typically less than 0.1 eV [13]. In addition, there are visible changes in the DOS maxima produced by interface bonding similar to that found for the $Fe/BaTiO_3$ interface [11].

The electronic structure at the Fermi energy (E_F) determines transport properties. Figure 3(a) shows the $\mathbf{k}_\parallel$-resolved local DOS for the middle and the interface Pt atoms at E_F. The features seen for bulk Pt in the left panel reflect the projection of the Pt Fermi surface on the two-dimensional Brillouin zone. In particular, the presence of the Fermi surface pockets along the [100], [010], and [001] directions forming ellipsoids in bulk Pt produce two superimposed "lenses" rotated by 90° and a circle near the $\bar{\Gamma}$ point ($\mathbf{k}_\parallel = \mathbf{0}$). These states are slightly deformed close to the interface [the right panel in Fig. 3(a)] and extended to the interface Ti and O atoms (not shown). These states dominate the tunneling conductance.

The presence of ferroelectricity in $BaTiO_3$ alters the electronic structure, producing a notable shift in the position of the DOS maxima at the interface, which ultimately affects the conductance. Figure 3(b) shows the $\mathbf{k}_\parallel$-resolved DOS for the interface Pt and Ti atoms at the left and right interfaces in a $Pt/BaTiO_3/Pt$ FTJ in the central part of the Brillouin zone. It is seen that the electronic states at the

FIG. 2 (color online). Local DOS in a $Pt/BaTiO_3/Pt$ tunnel junction as a function of energy. The results are for the $m = 4$ $BaTiO_3$ barrier in the paraelectric (a) and ferroelectric (b) states. The O_2 and Ti DOS in the middle TiO_2 monolayer are shown by the shaded area. In (b) the polarization is assumed to be pointing to the right, as in Fig. 1(b).

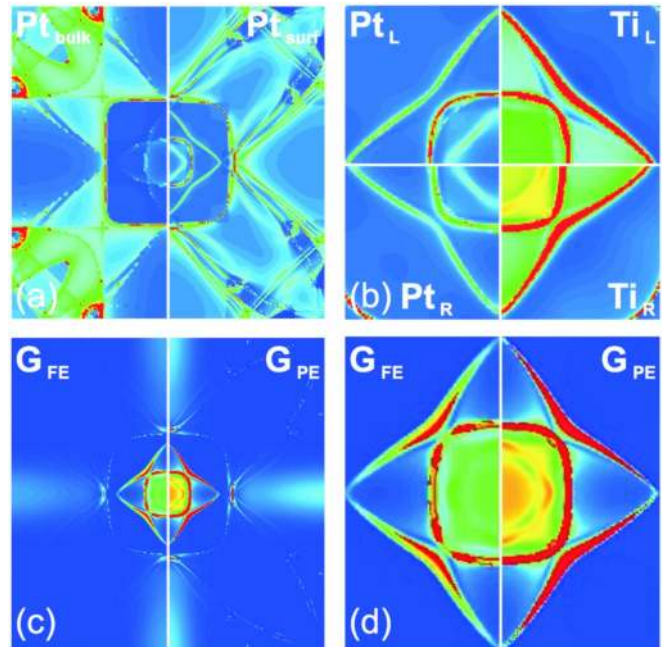FIG. 3 (color online). $\mathbf{k}_\parallel$-resolved DOS at the Fermi energy and conductance for a $Pt/BaTiO_3/Pt$ tunnel junction. (a) Pt bulk and Pt interface DOS for paraelectric (PE) $BaTiO_3$ in a half Brillouin zone; (b) local DOS for Pt and Ti interface atoms for ferroelectric (FE) $BaTiO_3$ near the $\bar{\Gamma}$ point; (c) conductance for PE and FE $BaTiO_3$; (d) same as (c) near the $\bar{\Gamma}$ point.

right interface are displaced closer to the $\bar{\Gamma}$ point compared to those at the left interface. This shift reflects the different electrostatic potentials at the two interfaces seen in Fig. 2(b). Since the transmission coefficient across the barrier depends strongly on $\mathbf{k}_\parallel$, this change in the DOS influences the conductance.

The conductance is calculated by considering a $BaTiO_3$ layer of given thickness m placed between two seminfinite Pt electrodes, using the TB-LMTO method and the principal-layer Green's function technique [25]. For $m = 4$ we find that the conductance per unit cell area changes from $G_{PE} \approx 17.0 \times 10^{-5} e^2/h$ to $G_{FE} \approx 2.9 \times 10^{-5} e^2/h$ when $BaTiO_3$ alters its state from paraelectric to ferroelectric. This implies that ferroelectric displacements produce a significant conductance change $G_{PE}/G_{FE} \approx 6$. The inspection of the $\mathbf{k}_\parallel$-resolved transmission in Fig. 3(c) indicates that the main contribution to the conductance comes from the area around the Brillouin zone center, replicating features in the DOS [Fig. 3(a), right panel]. This behavior is similar to that found for $Co/SrTiO_3/Co$ tunnel junctions [26] and is the consequence of a low decay rate in the barrier for the states lying close to the $\bar{\Gamma}$ point.

A closer look at the $\mathbf{k}_\parallel$-resolved transmission near the $\bar{\Gamma}$ point [Fig. 3(d)] indicates that transmission peaks are slightly deformed when the barrier is ferroelectric. This is due to the mismatch between the electronic states at the left and right interfaces induced by ferroelectric displacements [Fig. 3(b)]. For a paraelectric junction the matching of the DOS maxima at the two interfaces results in resonant transmission making the conductance much higher than that for a ferroelectric junction where the interfaces are asymmetric.

In practice, this resonant transmission may, however, be hindered due to disorder which is always present in real tunnel junctions [27]. In order to check the sensitivity of G_{PE}/G_{FE} to disorder, we calculated the conductance as a function of the imaginary part γ added to the energy, in the spirit of the approach used in Ref. [27]. We find that the conductance of the paraelectric (symmetric) junction is more sensitive to disorder. However, $\bar{\Gamma}$ remains substantial even at very large values of γ. In particular, for $\gamma = 0.01$ eV, which provides a correct order of magnitude for low-temperature conductivity of a metallic thin film, we find $G_{PE}/G_{FE} \approx 2.5$. This implies that the predicted effect may be observed in practice.

In addition to the shift of the electronic states at the two interfaces, polarization related atomic displacements cause a tetragonal distortion reducing symmetry. This alters the complex band structure of the insulator controlling electron tunneling [28]. Figure 4 shows the two lowest decay rates at E_F in paraelectric bulk $BaTiO_3$ (solid lines) [29]. The complex band structure of $BaTiO_3$ is similar to that of $SrTiO_3$ with two evanescent states of Δ_1 and Δ_5 symmetry having lowest decay rates [26]. The inset of Fig. 4 demonstrates that the states close to the center of the Brillouin zone have about the same rate of decay due to the low
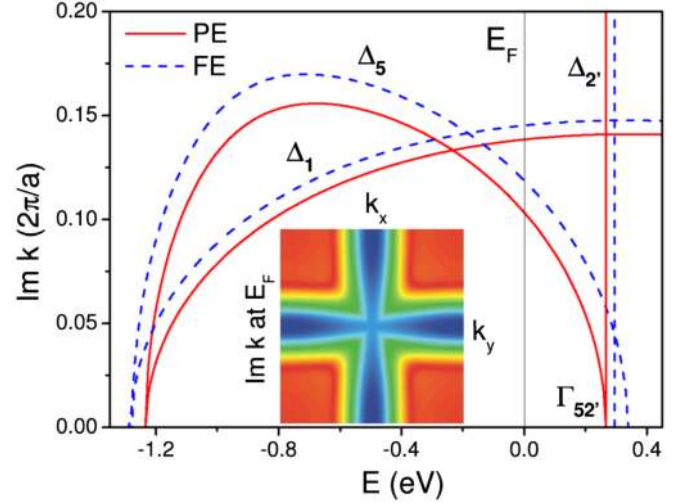

FIG. 4 (color online). Complex band structure $BaTiO_3$ in PE and FE states. The two lowest decay rates of the evanescent states of Δ_1 and Δ_5 symmetry are displayed. Ferroelectric distortion splits the $\Gamma_{52'}$ triplet into a doublet Γ_5 and a singlet $\Gamma_{2'}$. The Fermi level in the corresponding $Pt/BaTiO_3/Pt$ FTJ is shown by a vertical line. Inset shows the lowest decay rate as a function of $\mathbf{k}_\parallel$ in the two-dimensional Brillouin zone.

dispersion of the Ti-d bands in the [100] and [010] directions. In addition, Fig. 4 shows the change in the complex band structure resulting from ferroelectric displacements of atoms from their equilibrium positions (dashed lines). The structural change causes an increase of the band gap [30] and splits the triply degenerate lowest unoccupied state $\Gamma_{52'}$ into a doublet Γ_5 and a singlet $\Gamma_{2'}$ (see Fig. 4). This enhances the decay rates producing the conductance drop due to ferroelectricity in the barrier.

The evidence of the electroresistance effect predicted for a FTJ with different electrodes [13,14] can be obtained by analyzing the difference in the transmission across the left and right $Pt/BaTiO_3$ interfaces. It is known that, for not too thin barriers, the transmission function $T(\mathbf{k}_\parallel)$ of a tunnel junction may be factorized [31]

$$T(\mathbf{k}_\parallel) = t_L(\mathbf{k}_\parallel) \exp[-2\kappa(\mathbf{k}_\parallel)d]t_R(\mathbf{k}_\parallel). \quad (1)$$

Here t_L and t_R are the interface transmission functions (ITF) characterizing the left and right interfaces, $\kappa(\mathbf{k}_\parallel)$ is the lowest decay rate in the barrier (see the inset of Fig. 4), and d is the barrier thickness. The ITF is the transmission probability from the left or right electrode to the barrier across the interface for an electron with a given $\mathbf{k}_\parallel$. For a $Pt/BaTiO_3/Pt$ FTJ the two interfaces are not identical and therefore t_L and t_R are different. We can find the difference between the two by analyzing the density of metal induced gap states at distance x from the left (right) interface

$$|\psi_{L,R}(\mathbf{k}_\parallel)|^2 \propto t_{L,R}(\mathbf{k}_\parallel) \exp[-2\kappa(\mathbf{k}_\parallel)x]. \quad (2)$$

Figure 5 shows the density of metal induced gap states for $\mathbf{k}_\parallel = \mathbf{0}$ at the Fermi energy that reflects the asymptotic behavior of conductance in the limit of thick barrier. It is
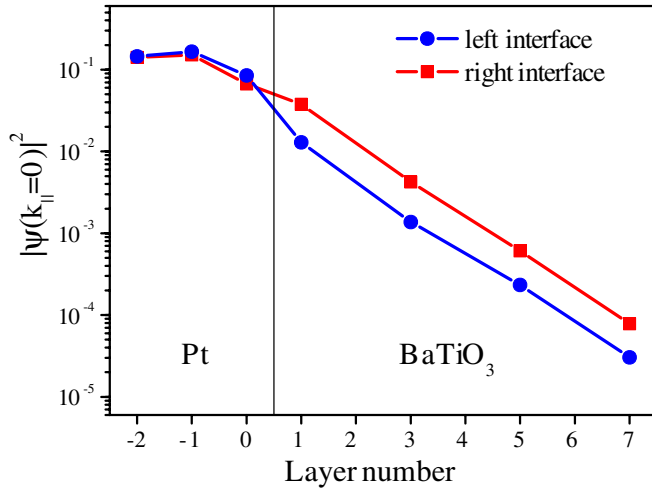
FIG. 5 (color online). Probability density $|\psi|^2$ for the state at $\mathbf{k}_{\parallel} = 0$ with the lowest decay rate for the left (circles) and right (squares) interfaces in a Pt/BaTiO$_3$/Pt FTJ at the Fermi energy. The results are obtained using VASP for a $m = 8$ BaTiO$_3$ barrier layer. Within BaTiO$_3$ $|\psi|^2$ is displayed on Ti atoms.

evident that the electron density induced in the gap by the Pt electrode through the right interface is a factor of 3 higher than the density induced through the left interface, i.e., $t_R/t_L \approx 3$. This implies that the transmission through the interface changes by a factor of 3 with polarization reversal. If an asymmetric FTJ had one such interface with the other being ferroelectrically dead, the resistance of the FTJ would change by a factor of 3.

Our results reveal from first principles two important mechanisms induced by ferroelectric switching affecting the tunneling conductance in FTJs: (i) change in the electrostatic potential and the bonding at the interface and (ii) change in the decay rates of the evanescent states in the barrier. The first alters the interface transmission function, while the second affects the attenuation constant in the barrier. These mechanisms may be regarded as microscopic interface effects and strain effects in the barrier which act in addition to the incomplete screening [14]. We hope that our theoretical predictions will stimulate further experimental studies of ferroelectric tunnel junctions.

[1] M. Dawber, K. M. Rabe, and J. F. Scott, Rev. Mod. Phys. **77**, 1083 (2005).
[2] J. F. Scott, J. Phys. Condens. Matter **18**, R361 (2006).
[3] G. W. Dietz et al., J. Appl. Phys. **82**, 2359 (1997); S. Zafar et al., Appl. Phys. Lett. **73**, 3533 (1998); L. Pintilie and M. Alexe, J. Appl. Phys. **98**, 123103 (2005).
[4] H. M. Chen, S. W. Tsaur, and J. Y. M. Lee, Jpn. J. Appl. Phys. **37**, 4056 (1998); P. Zubko, D. J. Jung, and J. F. Scott, J. Appl. Phys. **100**, 114113 (2006).
[5] I. Stolichnov et al., Appl. Phys. Lett. **73**, 1361 (1998).
[6] E. Y. Tsymbal and H. Kohlstedt, Science **313**, 181 (2006).
[7] D. D. Fong et al., Science **304**, 1650 (2004).
[8] C. Lichtensteiger et al., Phys. Rev. Lett. **94**, 047603 (2005).
[9] D. A. Tenne et al., Science **313**, 1614 (2006).
[10] J. Junquera and Ph. Ghosez, Nature (London) **422**, 506 (2003); N. Sai, A. M. Kolpak, and A. M. Rappe, Phys. Rev. B **72**, 020101 (2005); C. G. Duan et al., Nano Lett. **6**, 483 (2006).
[11] C. G. Duan, S. S. Jaswal, and E. Y. Tsymbal, Phys. Rev. Lett. **97**, 047201 (2006).
[12] G. Gerra et al., Phys. Rev. Lett. **96**, 107603 (2006).
[13] M. Y. Zhuravlev et al., Phys. Rev. Lett. **94**, 246802 (2005).
[14] H. Kohlstedt et al., Phys. Rev. B **72**, 125341 (2005).
[15] J. Rodríguez Contreras et al., Appl. Phys. Lett. **83**, 4595 (2003).
[16] M. Gajek et al., Nat. Mater., advance online publication 11 March (2007).
[17] P. W. M. Blom et al., Phys. Rev. Lett. **73**, 2107 (1994).
[18] R. Oligschlaeger et al., Appl. Phys. Lett. **88**, 042901 (2006).
[19] G. Kresse and D. Joubert, Phys. Rev. B **59**, 1758 (1999).
[20] We use the generalized gradient approximation, the energy cutoff of 500 eV for the plane wave expansion, and a $10 \times 10 \times 1$ grid for k-point sampling. All the structural relaxations are performed until the forces on atoms become less than 20 meV/Å.
[21] O. K. Andersen, Phys. Rev. B **12**, 3060 (1975); O. K. Andersen and O. Jepsen, Phys. Rev. Lett. **53**, 2571 (1984).
[22] We use atomic spheres of radii: $R_{Ba} = 2.20$ Å, $R_{Ti} = 1.30$ Å, $R_O = 0.96$ Å, and $R_{Pt} = 1.56$ Å. For space filling we introduce an empty sphere of radius $R_E = 1.06$ Å at each interface. The quality of this choice of the spheres is tested against VASP calculations.
[23] As was noted in Ref. [12], in this case the tetragonal state of BaTiO$_3$ becomes unstable at $T = 0$ K, so the studied BaTiO$_3$ barriers are artificially stabilized in the tetragonal phase.
[24] This is smaller than the experimental value of about 3.5 eV, which is due to the well-known deficiency of the local density approximation.
[25] J. Kudrnovský et al., Phys. Rev. B **62**, 15 084 (2000).
[26] J. Velev et al., Phys. Rev. Lett. **95**, 216601 (2005).
[27] J. P. Velev, K. D. Belashchenko, and E. Y. Tsymbal, Phys. Rev. Lett. **96**, 119601 (2006).
[28] P. Mavropoulos, N. Papanikolaou, and P. H. Dederichs, Phys. Rev. Lett. **85**, 1088 (2000).
[29] In this calculation BaTiO$_3$ is assumed to be cubic in the paraelectric state and tetragonal in the ferroelectric state.
[30] This effect is analogous to the strain-induced shifts of the conduction and valence band edges due to deformation potentials in insulators.
[31] K. D. Belashchenko et al., Phys. Rev. B **69**, 174408 (2004).